Hindawi Publishing Corporation
Shock and Vibration
Volume 2016, Article ID 2041671, 10 pages
http://dx.doi.org/10.1155/2016/2041671

Research Article

Development and Application of the Downhole Drilling String Shock-Absorption and Hydraulic Supercharging Device

Yongwang Liu, Zhichuan Guan, Hongning Zhang, and Bo Zhang

China University of Petroleum, Qingdao 266580, China

Correspondence should be addressed to Yongwang Liu; liuyongwang2003@163.com

Received 29 February 2016; Revised 7 August 2016; Accepted 18 August 2016

Academic Editor: Salvatore Strano

It is a hot topic for deep/ultradeep wells to improve rock-breaking efficiency and drilling speed by available downhole energy. Based on different downhole energies and working conditions, specialized plunger pump is proposed to convert longitudinal vibration of drilling string into rock-breaking energy. Technical design is developed to generate high-pressure water jet. And then a simulation model is built to verify feasibility of the technical design. Through simulation, the influence law of key factors is obtained. On this basis, this device is tested in several wells. The result indicates this device can increase drilling speed as much as 136%. Meanwhile the harmful vibration can be absorbed. The energy from drilling string vibration is of high frequency and increases as well depth and formation anisotropy increase. By reducing adverse vibration, this device is able to increase the drilling speed and the service life also meets the demand of field application. The longest working time lasts for more than 130 hours. The performance of this device demonstrates great application prospect in deep/ultradeep resources exploration. To provide more equipment support for deep/ultradeep wells, more effort should be put into fundamental study on downhole drill string vibration and related equipment.

1. Introduction

As more and more effort is put into deep petroleum resources exploration, deep/ultradeep wells are drilled in both new and old oil and gas fields [1–5]. Moreover, the well depth becomes deeper and deeper. However, the slow drilling speed limits the drilling of deep/ultradeep wells. To overcome this challenge, researchers have developed a number of tools to increase drilling speed, including downhole motor device, rotary percussion drilling tools, downhole hydraulic pulsed cavitation jet generators, and downhole torsional drilling tools [6–17]. Although these tools differ in working mechanisms, their energies are all from drilling fluid. Field practices proved that drilling fluid pressure loss increases as the well depth increases. In extreme cases, drilling fluid is only able to carry cuttings in ultradeep wells [18–20]. It is obvious that tools based on drilling fluid energy would not achieve good performance in such wells. Therefore it is essential and important to find new downhole energy to develop new speedup techniques and related equipment.

Research and field practice prove that increasing water jet pressure of drilling bit can improve drilling speed greatly [21–29]. So, two methods are proposed. First is to supercharge drilling fluid on ground. Second is downhole supercharging [30–33]. Supercharging on ground is complex and expensive. Therefore it is not widely applied. Downhole supercharging does not change current drilling technology and equipment. A supercharging device is installed above drilling bit. Part of the drilling fluid can be supercharged to over 100 MPa. Such high-pressure can help to break rock. The available downhole supercharging devices are powered by drilling fluid. These devices transport the whole drilling fluid energy to part of the drilling fluid. Limited by this mechanism, these devices need complex hydraulic transformation system. However, the downhole space is restricted and condition is not so good; complex hydraulic transformation system can hardly work. So up to now, there is still no downhole supercharging device that can increase jet pressure to 100 MPa when the drilling technology and equipment do not change although much effort has been put [34–39].

This paper analyzes the downhole energy resources and proposes specialized plunger pump to convert longitudinal vibration of drilling string into rock-breaking energy. Technical design is developed to generate high-pressure water jet.

And then a simulation model is built to verify feasibility of the technical design. Through simulation, the influence law of key factors is obtained. On this basis, this device is tested in several wells. Based on above analysis, downhole drilling string shock-absorption and hydraulic supercharging device is developed. The field application shows remarkable effect on improving drilling speed.

2. Available Downhole Energies

The characteristics of different downhole energies are important for finding an optimal downhole energy to propel device. Currently, available downhole energies include energy carried by downhole media and downhole natural energy.

2.1. Energy Transmitted by Cable. Cable is one of the most effective methods to carry energy into well. Downhole tools based on this energy include downhole motor drilling bit, downhole motor rotary percussion drilling bit, and laser drilling tools. Energy transmitted by cable has three advantages. First, the energy is not subjected to well depth or drilling fluid. Second, the downhole tool can be controlled from surface by adjusting energy. Third energy is stable and without limitation on the working hours. However, the failure probability will increase when this energy is applied. Also, the relatively high cost makes it hard to apply.

2.2. Downhole Battery. Downhole battery is a portable energy. Tools based on portable energy include rotary steerable drilling systems and new downhole motor rotary percussion drilling tool. This energy is mostly used to change the drilling fluid distribution and speed and eventually propel the downhole tool. This energy is convenient and can provide relatively stable energy, but it has some shortfalls. First, the energy provided is too small to provide for large-power downhole tools. Second, its limited working time prevents it from working long hours in the well. Third, it is sensitive to the working conditions and hardly able to work regularly when encountering high temperature formations.

2.3. Energy from Drilling Fluid. This method is one of the most widely used methods. Many tools have been developed upon this energy, including downhole screw drilling tool, turbine drilling tool, hydraulic rotary percussion drilling tool, and torsional impact drilling tool. However, the drawbacks can also not be ignored while it has many advantages. The main drawback is the significant reduction of available energy as well depth increases. Figure 1 shows the pipe pressure loss varies with the well depth under different fluid capacities. As shown in Figure 1, the pipe circulating pressure loss increases linearly with the well depth. So it is also restricted to increase the deep well drilling speed by using the drilling fluid energy.

2.4. Geothermal Energy. The geothermal energy has been exploited for more than three decades. However, there is still no example of direct using of geothermal energy in drilling. Formation temperature increases with the depth at approximately 1°C per 33 m, so the downhole temperature

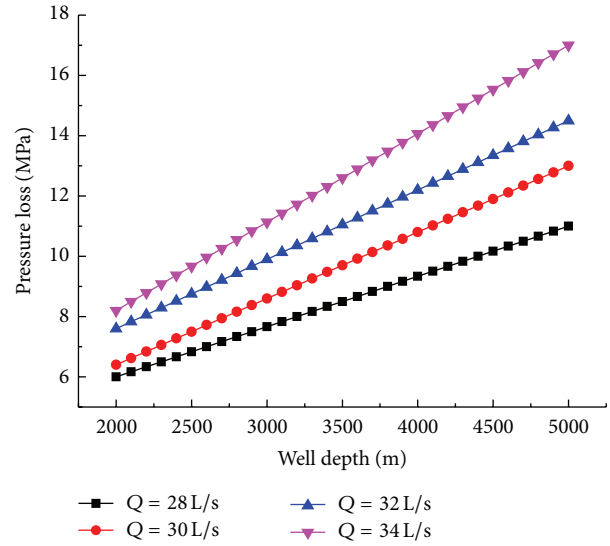

Figure 1: Impact of well depth on pipe pressure loss.

under 7000 m is as high as 210°C. If this energy can be converted into mechanical energy, the drilling speed will be increased greatly. More importantly, as this energy increases with the well depth, the deficiency of speedup energy in deep formations can also be overcome. Unfortunately, no application of geothermal energy has ever been reported in drilling devices or equipment yet.

2.5. Drill String Vibration. Drilling string vibration is caused by longitudinal, torsional, or lateral shock, especially when drilling in a soft-hard interbedded formation. Drilling string vibration is adverse to drilling operation. First, it prevents the uniform WOB increase and torque application, which causes the drilling bit to fail earlier than expected. Second, it aggravates the fatigue failure of the drilling string, particularly the connection between drill strings where thread piercing, thread gluing, and rupture frequently happen. Third, it damages surface equipment.

Experimental research and previous field tests demonstrate downhole WOB is exposed to high frequency and large-amplitude fluctuation. The fluctuation amplitude increases as the well depth. Although drilling string vibration is harmful, it can be converted into useful energy, which can provide reliable energy for drilling speedup if properly utilized.

3. Structure and Working Principle of Downhole Drilling String Shock-Absorption and Hydraulic Supercharging Device

3.1. Design Theory. The cutting teeth of drilling bit will be exposed to great transient impact force which eventually causes teeth breakup if high frequency and large-amplitude WOB fluctuation is directly applied to the drilling bit. The WOB will be passed to the drill bit by spring and a damping structure after installing a spring and a damping structure in the middle of the drill string or on the top of the drill bit.

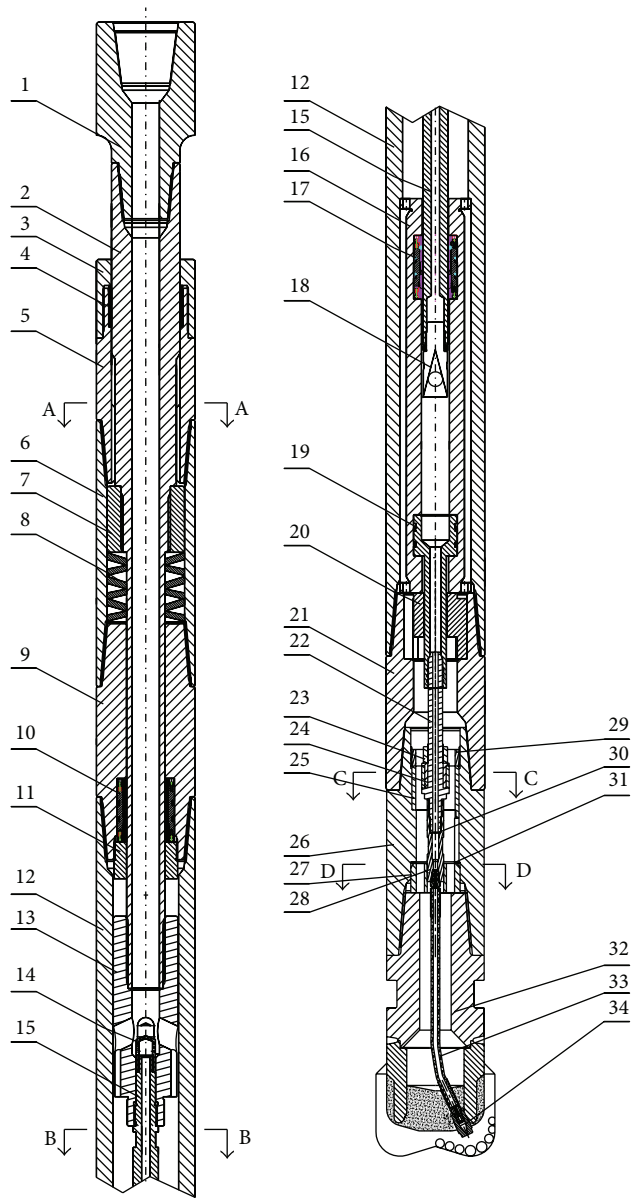

Figure 2: Structure of the downhole drill string shock-absorption and hydraulic supercharging device. Upper X-over 1; splined mandrel 2; sealing set 3; spring chamber upper seal assembly 4; splined outer barrel 5; spring protective barrel 6; splined check nut 7; spring 8; spring lower joint 9; spring chamber lower seal assembly 10; lower sealing set 11; supercharging assembly outer barrel 12; shunt pressure joint 13; drilling fluid filter 14; plunger 15; supercharging cylinder 16; hyperpressure seal assembly 17; inlet nonreturn valve 18; high-pressure runner 19; supported overflow frame 20; supercharger lower joint 21; metal hyperpressure drilling fluid runner 22; check nut 23; hexahedron 24; antitwist overflow structure 25; X-over 26; rigid pipe centralizer 27; hyperpressure drilling fluid runner extension pipe 28; locknut 29; pressure seal 20; adjustable retainer ring 31; drill frame 32; hyperpressure hose 33; hyperpressure frill fluid nozzle 34.

So the fluctuation is converted into elastic energy and damping power. This will largely attenuate the WOB fluctuation amplitude and extend the impact force duration. The counterforce of the internal liquid pressure in the plunger pump structure attenuates WOB fluctuation, just like a damper. This can convert the damping power into the internal liquid pressure of the plunger pump structure, thereby increasing the discharged liquid pressure from the plunger pump. The fundamental concept of the high-pressure jet generator is based on drill string vibration. This device uses the joint force of the spring and the plunger pump to attenuate WOB fluctuation and increase the discharged liquid pressure from the plunger pump.

3.2. Structure and Advantage. Figure 2 shows the structure of drilling string shock-absorption and hydraulic supercharging device.

This device is composed of a drilling string load transfer assembly, a torque-transfer and load-bearing assembly, an elastic recovery element assembly, a supercharger cylinder, a

hyperpressure drilling fluid-carrying assembly, and a drilling bit. The drilling string load transfer assembly consists of an upper X-over, a splined mandrel, a splined check nut, a shunt pressure joint, a drilling fluid filter, a plunger, and an inlet nonreturn valve. The torque-transfer and load-bearing assembly consists of a sealing set, a spring chamber upper seal assembly, a splined outer barrel, a spring protective barrel, a spring lower seal joint, a spring chamber lower seal assembly, a lower sealing set, a supercharger assembly outer barrel, a supported overflow frame, a supercharger lower joint, and an X-over. The supercharger cylinder consists of a supercharger cylinder and a hyperpressure seal assembly. The elastic recovery elements include springs, hydraulic springs, and other elements capable of achieving elastic recovery. The hyperpressure drilling fluid-carrying assembly consists of a high-pressure runner, a metal hyperpressure drilling fluid runner, a hyperpressure drilling fluid runner extension pipe, a hyperpressure hose, and a hyperpressure drilling fluid nozzle. The drilling bit is ordinary.

The supercharger cylinder is inside the torque-transfer. This two-part bearing keeps relatively stationary. The torque is transferred to the torque-transfer and load-bearing assembly through the collaboration of the splined on the splined mandrel, which in turn drives the drilling bit to rotate and break the rock. The WOB fluctuation causes the drilling string load transfer assembly to move back and forth when the drilling string vibrates longitudinally. When the WOB increases, the drill string load transfer assembly moves up and down relative to the torque-transfer and load-bearing assembly. The inlet nonreturn valve closes. The spring, together with the drilling fluid in the supercharger cylinder, receives the load and applies counterforce to stop this movement. This compresses the spring and the drilling fluid pressure in the supercharger cylinder increases, which eventually supercharges part of the drilling fluid. The supercharged drilling fluid is then transferred to the drilling bit and ejected out from drilling fluid nozzle installed on the drill bit to help break the rock. When WOB decreases, the compressed spring stretches. The drilling string load transfer assembly moves up relative to the torque-transfer and load-bearing assembly. The pressure in the supercharger cylinder is reduced. The inlet nonreturn valve opens and absorbs in constant-pressure drilling fluid to prepare for the next supercharging cycle.

The workflow of the drilling fluid is the drilling fluid flows through the cavity between the upper X-over and the cavity of the splined mandrel and then is divided into two parts at the shunt pressure joint. One part flows through the drilling fluid filter, plunger, and inlet nonreturn valve into the supercharger cylinder and is supercharged. The other part flows through the annulus between the supercharger assembly outer barrel and the plunger, the annulus between the supercharger assembly outer barrel and the supercharger cylinder, the annulus made up of the supported overflow frame runner, high-pressure runner, and supercharger lower joint, the overflow hole of the antitwist overflow structure, metal hyperpressure drilling fluid runner, the annular space between the hyperpressure drilling fluid runner extension pipe and the X-over inner hole, and the annular space between the hard pipe centralizer overflow hole, hyperpressure hose, and drill inner chamber down to the well bottom, where it is ejected out of the normal nozzle installed on the drilling string to serve as drilling fluid.

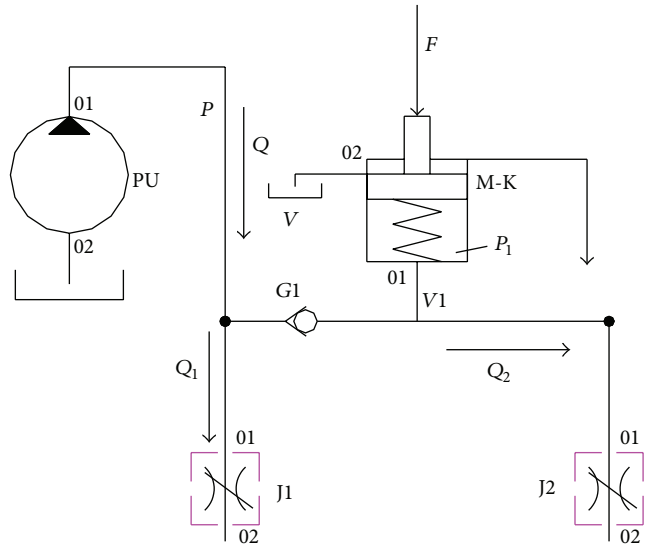

Figure 3: Working principle of the downhole drill string shock-absorption and hydraulic supercharging device.

The supercharged drilling fluid flows through the hyperpressure drilling fluid-carrying assembly that is composed of the high-pressure runner, metal hyperpressure drilling fluid runner, hyperpressure drilling fluid runner extension pipe, hyperpressure hose, and hyperpressure drilling fluid nozzle down to the well bottom, where it is ejected to help the drilling bit break the rock mechanically.

The merit of this design is to combine drilling string shock attenuation and fluid supercharging and then converts drilling string vibration energy into the pressure of the drilling fluid, which supercharges the well bottom and improves the rock-breaking efficiency. More importantly, this is achieved without changing existing drilling process and equipment or preventing regular circulation.

4. Simulation

Figure 3 shows the working principle of the downhole drilling string shock-absorption and hydraulic supercharging device, where F is the WOB wave power; M-K is the piston-spring recovery system; PU is the volume chamber; J1 is the flow inlet control nonreturn valve; J1 is normal drill nozzle; J2 is the hyperpressure nozzle.

As shown in Figure 3, the pressure control system is made of piston-spring element M-K and the supercharger. A numerical model is established according to continuous flow equation and vibration damping equation.

The kinetic equation of the piston is

$$Mx'' + Bx' + K\left(x + x_0\right) = F - \sum \Delta p \Delta A - \sum f, \quad (1)$$

where M is the piston mass, kg; B is the damping factor of elastic element, dimensionless; K is the elastic stiffness of elastic recovery system, N/mm; x is piston motion displacement, mm; x_0 is piston displacement in balance, mm; x' is piston motion speed, mm; x'' is piston motion acceleration, mm; F is the WOB wave force, N; ΔP is the piston internal pressure difference, pa; ΔA is the difference of bearing areas between upper and lower end faces of piston, mm^2; f is the frictional resistance, N.

Only consider the resistance from the combined seal assembly and ignore the viscous resistance of the drilling fluid, so the frictional resistance is expressed as

$$f = \mu\pi DLF_N, \tag{2}$$

where μ is the coefficient of kinematics friction, dimensionless; D is the combined seal outer diameter, mm; L is the combined seal length, mm; F_N is the pressure, N.

According to the mass conservation for a control volume V_i, the sum of inflow and outflow is zero. Considering the fluid compressibility and system leakage, a flow continuity equation is established for the internal supercharger cylinder of the device:

$$\frac{dp_1}{dt} = \frac{K}{V - Ax}\left(Q_1 - Q_2 + Ax'\right) - c_L\Delta p, \tag{3}$$

where P_1 is the pressure inside the hydraulic cylinder, Pa; K is the bulk elastic modulus of mud, Pa; A is the piston area, m^2; V is the hydraulic cylinder volume, m^3; Q_1 is the input flow inside the hydraulic cylinder, m^3/s; Q_2 is the output flow inside the hydraulic cylinder, m^3/s; C_L is the leakage coefficient, dimensionless; Δp is the internal-to-external pressure difference of the hydraulic cylinder, Pa.

In Figure 3, J1 is the inlet flow control nonreturn valve, where the inlet flow varies with the internal-to-external pressure difference of the nonreturn valve. On this basis, we have a pressure-flow equation of the control nonreturn valve:

$$\begin{aligned} Q_d &= c_d w \frac{A_d \Delta p}{K_d}\sqrt{\frac{2\Delta p}{\rho}}, \\ R_G &= c_d w x_{\max}\sqrt{\frac{2}{\rho}}. \end{aligned} \tag{4}$$

And then

$$Q_1 = \begin{cases} 0, & \Delta P \le 0, \\ R_G \dfrac{A_d}{K_d x_{\max}}\sqrt{\Delta p^3}, & 0 < \Delta P < P_d, \\ R_G\sqrt{\Delta P}, & \Delta P \ge P_d, \end{cases} \tag{5}$$

where R_G is liquid conductivity of the nonreturn valve when stabilized at the largest position; p_d is pressure drop of the nonreturn valve at the largest position.

In Figure 3, PU is the volume chamber. According to mass conservation, a flow continuity equation can be established:

$$\frac{dp}{dt} = \frac{K}{V}\left(Q - Q_1 - Q_2\right), \tag{6}$$

where p is the pressure inside the volume chamber, Pa; K is the bulk elastic modulus of mud, Pa; V is the volume of the volume chamber, m^3; Q is the displacement of the drilling fluid, m^3/s; Q_1 is the output flow from a normal drill nozzle, m^3/s; Q_2 is the output flow from a hyperpressure nozzle, m^3/s.

In Figure 3, J1 is the normal drilling bit nozzle and J2 is the hyperpressure nozzle. According to the small orifice equation, an equation can be got:

$$Q = c_d\frac{\pi}{4}d^2\sqrt{\frac{2\Delta p}{\rho}}, \tag{7}$$

where Q is the outlet flow, m^3/s; c_d is the flow coefficient, dimensionless; d is the equivalent diameter of the nozzle, mm; Δp is the pressure drop of the nozzle, Pa; ρ is the density of the drilling fluid, kg/m^3.

4.1. Simulation Model. Figure 3 shows the simulation curve of the downhole drilling string shock-absorption and hydraulic supercharging device. The solid lines are the output pressure curves of the device. The broken lines are the piston motion displacement curves. As the plunger moves up and down (positive when up and negative when down), its displacement presents sine periodical fluctuation. In one cycle, the plunger starts moving down from the initial position ($x = 0$). The pressure in the supercharger cylinder rises synchronously. When the plunger moves to the balanced position ($x = 0.13$ m), the pressure in the supercharger cylinder comes to the peak (146 MPa). The plunger continues to move down, so the pressure in the supercharger cylinder starts to drop. When the plunger reaches the maximum displacement ($x = 0.2$ m), the pressure in the supercharger cylinder drops to the normal pressure (close to the pressure in the drill string). This is the end of the supercharging cycle. The plunger starts to move up. At this time, the drilling fluid inside the drilling string flows into the supercharger cylinder. Due to cross-sectional effect of the runner, the pressure in the supercharger cylinder is lower than pressure in the drilling string. When the plunger reaches the minimum displacement ($x = 0.05$ m), the low-pressure fluid suction process comes to an end. This is the end of one working cycle of this device.

According to Figure 4, the simulation result indicates this device is able to supercharge part of the drilling fluid to 100 MPa. The pressure of this device is unsteady pressure. According to the working mechanism, the rock-breaking water power is associated with the structural parameters of this device and the diameter of the hyperpressure nozzle. To get the influencing law of these factors, the effects of these factors are analyzed to optimize the parameters.

4.2. Effect Law of Hyperpressure Nozzle Diameter on Device Working Behavior. The hyperpressure nozzle is the actuator of the hyperpressure jet ejector. Its equivalent diameter determines the ejective pressure. As shown in Figure 5, the maximum pressure of the device gradually reduces as the nozzle diameter increases. The effective rock-breaking water power depends on the elastic stiffness level. The effective rock-breaking water power gradually increases as the nozzle

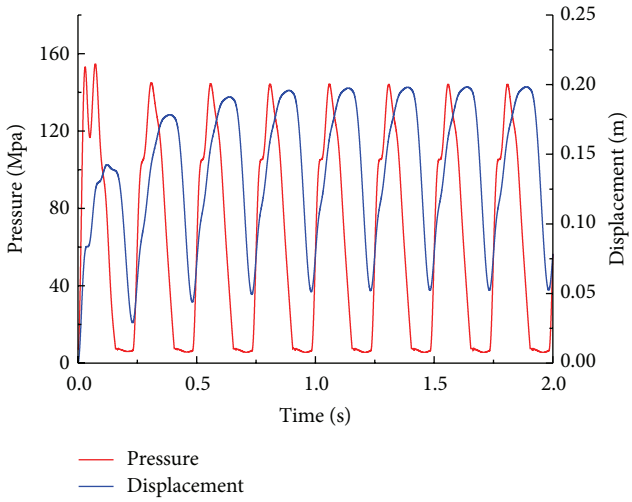

Figure 4: Simulation curve of the working behavior of the device.

diameter increases when the elastic stiffness is 0.5 KN/mm. But when the nozzle diameter is larger than 3 mm, this increase starts to decline. When the elastic stiffness is higher than 1 KN/mm, the effective rock-breaking water power increases first and then reduces as the nozzle diameter increases. Rock-breaking water power reaches its maximum when the nozzle diameter is 3 mm. This is because the maximum pressure of the device reduces slowly as the nozzle diameter increases when elastic stiffness is at smaller level. As the elastic stiffness increases, its maximum pressure reduces more quickly.

4.3. Effect Law of Elastic Modulus on Device Working Behavior. The piston and elastic elements of the device compose piston-spring damping system together. The resistance is too big for supercharging to go back to its original position if the elastic modulus of the elastic system is too large. If its elastic modulus is too small, the restoring force of the piston in its upward movement will be too small for it to get back to the expected position. Therefore, elastic modulus is also one of the important structural parameters.

As shown in Figure 6, the maximum pressure and effective rock-breaking water power of this device both decrease gradually as the elastic stiffness increases. However, the reduction differs under different nozzle diameters and increases as the nozzle diameter increases. Hence, the device should choose an elastic recovery system with small elastic stiffness with a prerequisite that adequate restoring force is provided for the piston.

5. Field Test and Speedup Result Analysis

Field tests were conducted on the second section well intervals with a diameter of Φ311.1 mm in Well ZG10-58, Luo69 and KS502, and KS502. The longest downhole working duration was 140.76 h. The longest drilling footage was 745.1 m. Encouraging speedup result was achieved from all the three wells.

5.1. First Test Well. The first field test of this device was conducted on the second-section Φ311.1 mm interval of ZG10-58 well. This well is in Shengli Oilfield. Design depth of this well is 4 885 m. The test interval is 3 457.5~3 482.5 m. The formation was mesozoic. The middle and upper parts mainly consist of grayish-white psephitic sandstone of different thickness. It is interbedded with pinkish or brownish red mudstone. The lower part is coal measure formation that contains carbonaceous mudstone, coal measure, and gray mudstone and locally interrupted by thick-layered gray psephitic sandstone.

The drilling string combination was Φ311.1 mm downhole hyperpressure PDC drill + JZZY-1 supercharger + 3 Φ228.6 mm drill collars + 3 Φ203.2 mm drill collars + 6 Φ177.8 mm drill collars + Φ127.0 mm drill string. The drilling parameters were WOB: 60~100 kN; rotary table speed: 75 r/min; displacement: 40 L/s; drilling fluid density: 1.43 g/cm^3.

In this test, this device worked in the well for 8.6 hours. Subtracting the time of downhole shaping and circulation, the net working time was 3 hours. The drilling footage was 25 m.

Because no record of an adjacent well has the same diameter as this well, the drilling record in the upper adjacent interval of this test well was used for comparison. This interval is in the same formation. For the interval before the device was tripped in comparison interval, the drill combination is Φ311.1 mm roller drill + Φ228.6 mm shock absorber + 3 Φ228.6 mm drill collars + 3 Φ203.2 mm drill collars + 6 Φ177.8 mm drill collars + Φ127.0 mm drill string. The drilling parameters are as follows: WOB: 200~220 kN; rotary table speed: 80 r/min; displacement 42 L/s; drilling fluid density: 1.42 g/cm^3.

Figure 7 shows the measured drilling speed of the test interval and the comparison interval. The average drilling time of the comparison interval is 50 min/m. In the 25 m footage before this device is applied, the average drilling time is as high as 90.10 min/m, compared to the 9.67 min/m average in the test interval. Compared with the comparison interval, the average drilling speed was increased by 417%. Compared with the adjacent 25 m comparison interval, the mechanical speed was increased by 831%. Besides, available drilling practices in this area have proved that a PDC drilling bit is not suitable for mesozoic formations. The success of this test also shows the possibility of using PDC drill bits in this area to increase the drilling speed.

5.2. Second Test Well. This field test was in the second-section Φ311.1 mm interval of Well Luo 69 in Shengli Oilfield. This well has design depth of 3200 m. The test interval is 2200~2910 m. The drilling formation is Dongying Formation to Shahejie Formation Sha-4 member. The drilling string combination was Φ311.1 mm hyperpressure PDC drill + JZZY-1 supercharger + 6 Φ203.3 mm drill collars + 9 Φ177.8 mm drill collars + Φ127.0 mm drill string. The drilling parameters were WOB: 60~100 kN; rotary table speed: 110~120 r/min; displacement: 45~48 L/min; pump pressure: 17~18 MPa.

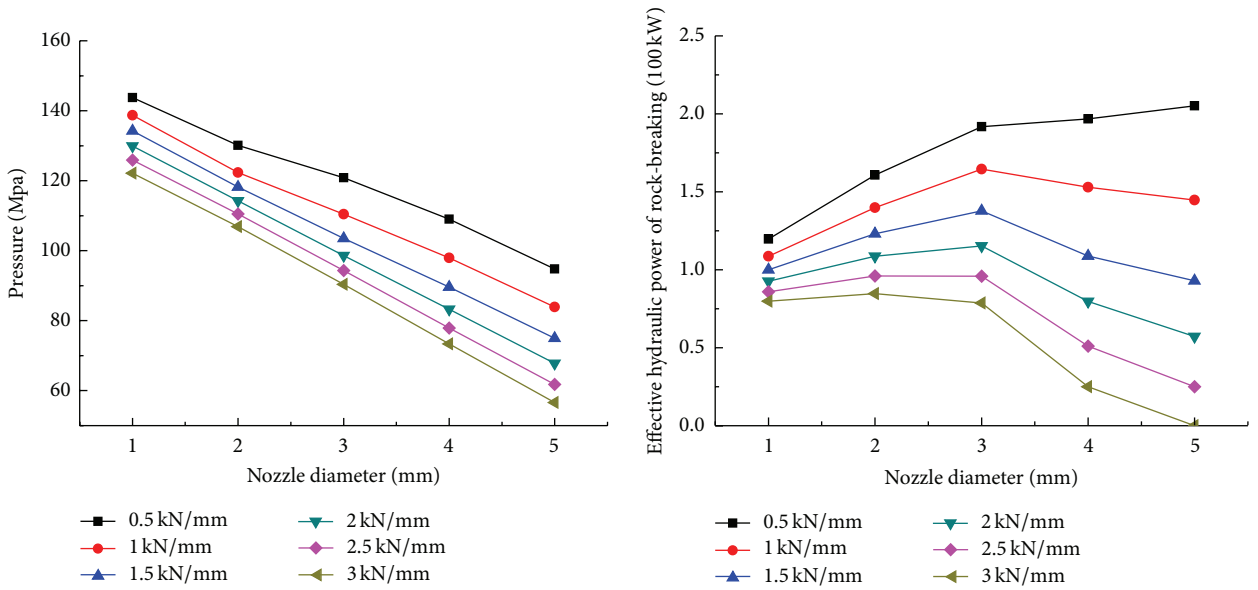

Figure 5: Effect law of hyperpressure nozzle diameter on device working behavior.

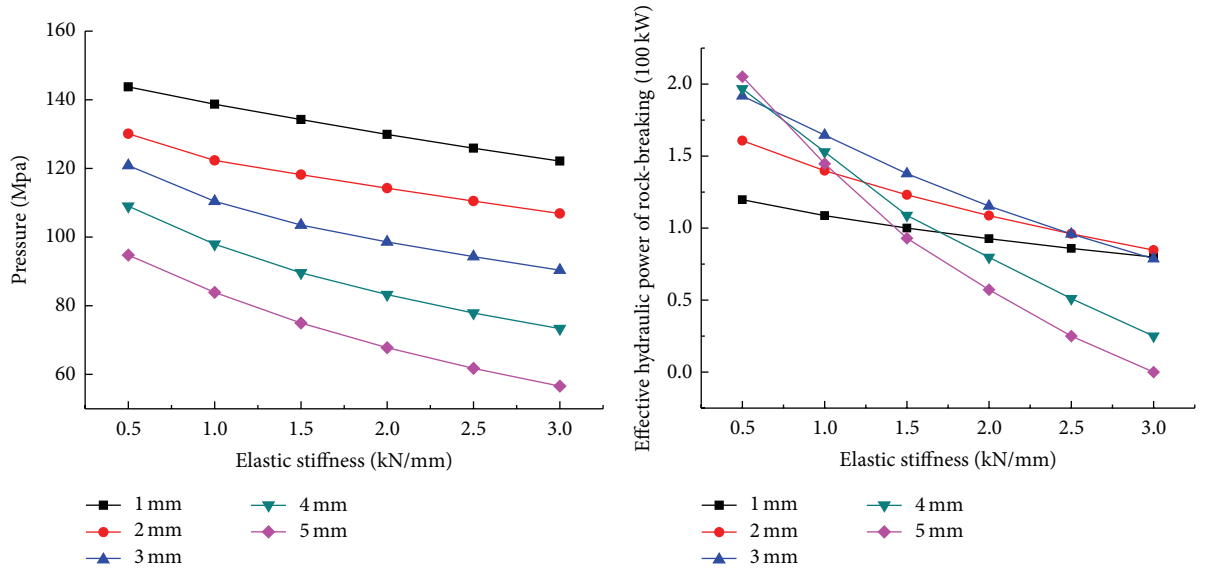

Figure 6: Effect law of elastic stiffness on device working behavior.

This device worked downhole for 93.7 hours. The net working time was 69 hours. The continuous drilling footage was 710 m.

The test interval in Well Luo 69 is compared with interval of the adjacent Luo 68, which used virtually the same drilling string combination and drilling parameters as Luo 69. The drilling bit is PDC. The test well and compared well are in the same formation and Table 1 compares the average drilling speed of the test well (Luo69) and the comparison well (Luo68). From this table, the average drilling speed of Luo 69 is increased by 85.4% compared with Luo 68. Obviously, the downhole drilling string shock-absorption and hydraulic supercharging device can greatly increase the mechanical drilling speed, especially when it comes to deep hard formation.

5.3. Third Test Well. The third test was conducted in Well KS502. The formations have low workability and contain a lot of pebbly intervals. From starting drilling till today, merely 1966 m drilling footage has cost 20 drilling bits. When pulled out of the well, the drilling bits have low newness and heavy abrasion. Furthermore, this well has excess formation dip angle and is prone to deflection.

The formation of this test well is Neozoic Neogene Kuche Formation. The formation lithologies mainly include granule and gray pebbly sandstone, interrupted by muddy siltstone

Table 1: Comparison of average mechanical drilling speeds of Luo69 and Luo68 within same well intervals.

Formation	Well interval/m	Avg. mechanical drill speed/(m·h^{-1})		Relative speedup rate, %
		Luo68	Luo69	
Dongying	2200~2510	8.86	20.91	136
Sha-1	2510~2750	8.90	10.60	19
Sha-2	2750~2830	5.02	6.52	30
Sha-3	2830~2850	3.57	5.96	70
Sha-4	2850~2910	1.92	6.78	254
Whole test interval	2200~2910	6.19	11.49	85.8

Table 2: Comparison of mechanical drilling speeds into siltstone and mudstone in adjacent well intervals speeds into siltstone and mudstone.

Speed comparison	Drilling method	Well depth/m	Lithology	Speed/m/h	Speedup comparison/%
Test interval	PDC + downhole shock-absorption and hydraulic supercharging device	1794–1848	Silty mudstone, brown mudstone	**3.84**	**+12**%
Comparison interval	PDC + Power-V	1489–1673		**3.43**	

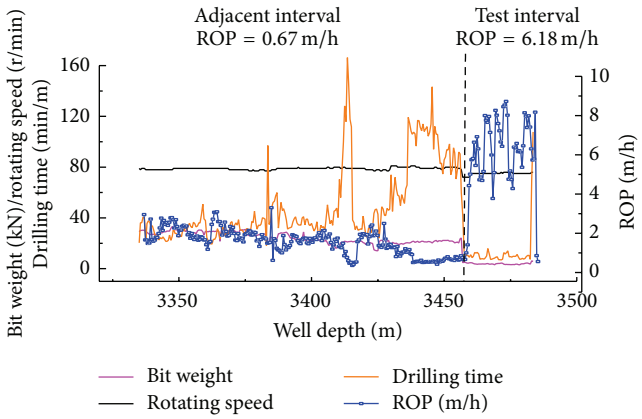

Figure 7: Field test result analysis of ZG10-58 well.

and brown mudstone. The test interval is 173 m, including 8 m granule with more than 90% gravel, 31 m siltstone with 65%–90% gravel, 7 m psephitic sandstone with 30%–65% gravel, and 59 m pebbly fine sand with 20%–30% gravel. The other intervals are predominantly muddy siltstone and silty mudstone, with 31 m muddy siltstone, 33 m silty mudstone, and 4 m brown mudstone.

Drilling Bit. There is best T1665GY, with nozzle combination: W16 ∗ 4 + W14 ∗ 4.

Drilling Combination for This Test. It consists of Φ335 drill + Φ228 downhole drill string shock-absorption and hydraulic supercharging device + Φ228DC + Φ334 centralizer + float valve + no magnetic drill collar + Φ334 centralizer + Φ228DC ∗ 2 + Φ203DC ∗ 14 + Φ203 drilling jar + Φ203DC ∗ 3 + Φ139HWDP ∗ 14 + Φ139DP.

Drilling Fluid Type. Drilling fluid is potassium chloride polysulfide drilling fluid system. The drilling fluid relative density is 1.7~1.75 g/cm^3. The viscosity is 65–75 s. The plastic viscosity is 30–40 MPA·s.

The device was placed in 1794 m and tripped out in 1966 m. The downhole working time was 133 hours. The net drilling time was 86.8 hours. The total footage was 173 m. When pulled out from well, the tool remained visually integral with no observable damage.

From 1498 to 1678 m, a PDC drilling bit was used in conjunction with Power-V. The drilling bit was GP1635. The borehole size was Φ335 mm. The drilling interval contains mudstone and silt intervals as well as gritstone intervals. This interval is adjacent to the drilling interval where this device is applied with best PDC drilling bits. The bit is identical (both are 6-blade and 16 mm polycrystalline diamond compacts) and borehole diameter is same too. The two intervals are therefore comparable for mechanical speed comparison according to the lithology and formation.

By comparison of Tables 2 and 3, the mechanical drilling speed is 12% higher than the adjacent interval when the WOB of the test interval is far smaller than the adjacent interval. In the gritstone interval, the speed of the test interval is 80% higher than the adjacent interval. It is noted that the average gravel ratio of the test interval was higher than 60% in the comparison of gritstone intervals, while the comparison interval was around 30%.

Adjacent wells close to KS502 are KS5 and KS501, but these wells are structurally different from the test well. For the same depth, a 444.5 m drill bit was used for both KS5 and KS501. Though the drilling size is different, the drilling result is still indicative. Table 4 compares the mechanical drilling speed of KS502 and the adjacent wells.

By comparing the drilling speed with the adjacent wells, the speed of test well KS502 is 39% higher than the adjacent KS5 and 75% higher than KS501 in the near interval of the same formation. Though the borehole sizes are different, this comparison can still indicate the speedup effect of the downhole drill string shock-absorption and hydraulic supercharging device.

Table 3: Comparison of speeds into siltstone in adjacent well intervals.

Speed comparison	Drilling method	Well depth/m	Lithology	Speed/m/h	Speedup comparison/%
Test interval	PDC + downhole shock-absorption and hydraulic supercharging device	1848–1966	Granule, siltstone, psephitic sandstone (with more than 60% gravel)	**1.44**	**+80%**
Comparison interval	PDC + Power-V	1674–1678	Psephitic sandstone (with around 30% gravel)	**0.8**	

Table 4: Comparison of mechanical drilling speed of KS502 with adjacent wells.

Well ID number	Interval/m	Formation	Drill model	Speed/m/h	Speed comparison
KS502	1794–1966	Kuche	T1665GY	2	
KS5	1892–2011		M1665SSCR	1.44	+39%
KS501	1868–1988		CK506DKG	1.14	+75%

As observed from the drilling data of the three test wells, the downhole drill string shock-absorption and hydraulic supercharging device is able to increase the drilling speed under the same drilling conditions. This device has stable function and reliable structure. Its service life is well qualified for extensive field application. In addition, the field test also confirms the superior shock-absorption effect of this device. When drilling into hard and complex formations, the violent vibration of drilling floor caused by drilling bounces was also mitigated.

6. Conclusions

(1) The drilling string vibration is absorbed to drive supercharging drilling fluid. This idea integrates drilling string shock-absorption with downhole drilling fluid supercharging. Accordingly, a downhole drilling string shock-absorption and hydraulic supercharging device was developed.

(2) Compared with previous downhole supercharging devices, the downhole drilling string shock-absorption and hydraulic supercharging device is more suitable to increase jet pressure in adverse downhole environment. It has simple structure and less vulnerable parts, so it can achieve longer service life.

(3) Field tests indicate that this device is able to increase the drilling speed and reduce drilling string vibration. It is feasible to use drilling string longitudinal vibration to increase downhole drilling fluid pressure. The device based on drilling string vibration is worthy of further studies. Development and promotion of this device will provide powerful support for safe, efficient drilling in deep and ultradeep wells.

(4) Further efforts are needed to investigate the formation suitability of this device, thus improving its reliability and gradually extending its application. Besides, this study has also opened the door to the application of drill string vibration in the speedup field. It can be expected that this energy will be used more extensively as the research goes deeper.

Competing Interests

The authors declare that they have no competing interests.

Acknowledgments

The authors would like to express their gratitude to the National Program on Key Basic Research Project of China (973 Program) (Grant no. 2010CB226706), the National Science and Technology Major Project of the Ministry of Science and Technology of China (Grant no. 2011ZX05021-001), and the National Science and Technology Major Project of the Ministry of Science and Technology of China (Grant no. 2011ZX05005-006-007HZ).

References

[1] C. Tinggen and G. Zhichuan, *Drilling Engineering Theory and Technology*, Petroleum University Press, Dongying, China, 2006.

[2] W. C. Maurer, *Advanced Drilling Techniques*, The Petroleun Publishing Company, Tulsa, Okla, USA, 1980.

[3] T. J. Labus, *Fluid Jet Technology: Fundamentals and Applications*, Water Jet Technology Association, Saint Louis, Miss, USA, 1995.

[4] T. J. Labus and G. A. Savanick, *An Overview of Waterjet Fundamental and Application*, Waterjet Technology Association, Saint Louis, Miss, USA, 2001.

[5] L. Gensheng, W. Zhiming, and H. Yongtang, "Numerical simulation of flowing field of high pressure jet impinging bottom-hole," in *Proceedings of the 7th Pacific Rim International Conference on Water Jet Technology*, Jeju, South Korea, October 2003.

[6] Z. Zhiyun, L. Gensheng, S. Huaizhong et al., "Experiment study on ultra-deep well Hydraulic pulsating-cavitating water jet drilling," *Petroleum Drilling Techniques*, vol. 37, no. 4, pp. 11–14, 2009.

[7] C. Hai, W. Jiachang, and Y. Benling, "Present situation research on pressurization at bottom hole technology about jet drilling home and abroad," *Oil Field Equipment*, vol. 37, no. 6, pp. 34–38, 2008.

[8] C. Yongduo, L. Jitai, X. Jibiao et al., "Research on enhancing drilling speed by using ultra-high pressure jet stream in bottom

hole," *Drilling & Production Technology*, vol. 31, supplement 1, pp. 6–10, 2008.

[9] Z. Wenhua, W. Zhiming, and Z. Yongzhong, "FEM calculation on rock breaking process by high pressure jet impact," *Petroleum Drilling Techniques*, vol. 34, no. 1, pp. 10–12, 2006.

[10] L. Hongmin, Z. Mingliang, P. Xin et al., "Downhole boost pressure drilling technology and the road ahead," *Oil Drilling & Production Technology*, vol. 20, no. 3, pp. 20–24, 1998.

[11] W. Taiping, C. Guangcun, L. Weigang et al., "Study on domestic & foreign ultra-high pressure jet drilling technique," *Petroleum Drilling Techniques*, vol. 31, no. 2, pp. 6–8, 2003.

[12] S. D. Veenhuizen, D. L. Stang, D. P. Kelley, J. R. Duda, and J. K. Aslakson, "Development and testing of downhole pump for high-pressure jet-assist drilling," SPE/IADC 38581, Society of Petroleum Engineers, 1997.

[13] J. J. Kolle, R. Otta, and D. L. Stang, "Laboratory and field testing of an ultra-high-pressure jet-assisted drilling system," SPE/IADC 22000, 1991.

[14] Z. Wenhua and L. Ling, "The influence factors of down—hole boost overpressure jet drilling," *Drilling & Production Technology*, vol. 26, no. 4, pp. 13–22, 2003.

[15] L. Zhimin, "Downhole fuidic supercharging device," *Foreign Petroleum Machinery*, vol. 6, no. 2, pp. 17–21, 1995.

[16] W. Deyu, "The structure of downhole supercharging device," *Journal of Southwest—China Petroleum Institute*, vol. 17, no. 3, pp. 109–112, 1995.

[17] W. Yajuan, "Theory discussion on the design of downhole supercharging device," *Journal of Shengli Oilfield Staff University*, vol. 15, no. 4, pp. 8–10, 2001.

[18] W. Deyu and H. Dongsheng, "Power analysis of downhole static pressure unit," *Journal of Southwest—China Petroleum Institute*, vol. 17, no. 1, pp. 115–119, 1995.

[19] Z. Wenhua, W. Zhiming, W. Xiaoqiu et al., "Design of jet type down-hole supercharger," *China Petroleum Machinery*, vol. 33, no. 11, pp. 32–33, 2005.

[20] Z. Wenhua, W. Zhiming, and W. Jiachang, "Experimental study on downhole jet boosting device," *China Petroleum Machinery*, vol. 33, no. 12, pp. 16–17, 2005.

[21] X. Liang, W. Zhiming, and L. Bangmin, "Numerical study of flow field for fuidic downhole boost compressor," *Petroleum Drilling Techniques*, vol. 38, no. 6, pp. 79–83, 2010.

[22] S. Wei, S. Feng, Z. Chongzhen et al., "Systematic design for a downhole centrifugal supercharging device," *China Petroleum Machinery*, vol. 34, no. 3, pp. 36–38, 2006.

[23] M. Qingguo, "The discussion on using screw pump as supercharging device," *Oil Drilling & Production Technology*, vol. 19, no. 2, pp. 50–51, 1997.

[24] A. Chi, Z. Rongxing, W. Zhixiang et al., "Whole structural design of the diaphragm pressure converter used in bottom-hole," *Journal of Daqing Petroleum Institute*, vol. 25, no. 1, pp. 89–91, 2001.

[25] A. Chi, L. Shibin, Z. Rongxing et al., "Calculating methods of principal structure parameters of diaphragm pressure converter," *Journal of Daqing Petroleum Institute*, vol. 25, no. 1, pp. 92–94, 2001.

[26] W.-Z. Wei, Z.-C. Guan, Y.-W. Liu, and Y.-C. Shi, "Experimental study on longitudinal vibration characteristics of pendulum assembly in straight hole," *Journal of China University of Petroleum (Edition of Natural Science)*, vol. 31, no. 2, pp. 60–68, 2007.

[27] G. Zhichuan, S. Yucai, and X. Yan, "Research on motion state of bottom hole assembly and the evaluation method of drilling tendency," *Petroleum Drilling Techniques*, vol. 33, no. 5, pp. 24–27, 2005.

[28] G. Zhichuan, W. Yifa, and J. Yanxin, "Experimental research on motion behavior of bottom drill string in straight hole," *Acta Petrolei Sinica*, vol. 24, no. 5, pp. 102–106, 2003.

[29] S. Yucai, W. Jun, Z. Jiang et al., "Research on backward whirling mechanism of bottom drillstring," *Petroleum Drilling Techniques*, vol. 35, no. 5, pp. 43–45, 2007.

[30] W. Wenzhong, G. Zhichuan, L. Yongwang et al., "Correlation experimental study on weight on bit (WOB) fluctuation characteristics of pendulum assembly and unbalanced assembly," *Journal of Oil and Gas Technology*, vol. 30, no. 1, pp. 157–160, 2008.

[31] X. Yan and G. Zhichuan, "Mechanical analysis of bottom drilling strings while using eccentric bits," *Petroleum Drilling Techniques*, vol. 30, no. 6, pp. 9–11, 2002.

[32] L. Yongwang, G. Zhichuan, W. Wenzhong et al., "Experimental study on rotary characteristics of bottom pendulum assembly," *Drilling & Production Technology*, vol. 31, no. 5, pp. 27–29, 2008.

[33] S. Yucai, G. Zhichuan, X. Yan et al., "Optimizing the design of bottom-hole assembly in deviation control by the trend angle of deviation," *Petroleum Drilling Techniques*, vol. 32, no. 5, pp. 10–12, 2004.

[34] S. Yucai, Y. Yanyan, and W. Chunfang, "Setting up a simulate device on motion behavior of bottom-hole assembly according to similitude principles," *Journal of Guangxi University: Natural Science Edition*, vol. 31, supplement 1, pp. 159–162, 2006.

[35] S. Yucai, W. Jun, and G. Zhichuan, "Research on whirling mechanism of bottom drillstring and its rules by inner simulated experiments," *Journal of Guangxi University*, vol. 32, no. 2, pp. 126–129, 2007.

[36] C. Daxian, *Mechanical Design Manual: Spring, Lifting Transportation Parts, Hardware*, Petroleum Industry Press, Beijing, China, 2004.

[37] L. Yingmin, *Material Mechanics*, Petroleum University Press, Dongying, China, 1993.

[38] J. Oppelt, E. Christensen, C. Chur et al., "New concepts for vertical drilling of boreholes," SPE/IADC 21905, 1991.

[39] A. Calderoni, A. Savini, J. Treviranus et al., "Outstanding economic advantages based on new straight-hole drilling device proven in various oilfield locations," SPE 56444, 1999.